Available online at www.sciencedirect.com
SCIENCE DIRECT
Tectonophysics 422 (2006) 89–98
TECTONOPHYSICS
www.elsevier.com/locate/tecto

Late Paleoproterozoic extension and a paleostress field reconstruction of the North China Craton

Guiting Hou [a,b,*], Chuancheng Wang [a], Jianghai Li [a], Xianglin Qian [a]

[a] *The Key Laboratory of Orogenic Belts and Crustal Evolution, School of Earth and Space Sciences, Peking University, Beijing 100871, China*
[b] *Research School of Earth Science, Australian National University, ACT 0200, Australia*

Received 30 August 2005; received in revised form 6 May 2006; accepted 10 May 2006
Available online 10 July 2006

Abstract

Mafic dyke swarms and aulacogens are major anorogenic extensional events in the Late Paleoproterozoic North China Craton (NCC). The N–NNW mafic dyke swarms are widespread in the NCC, whose ages span between 1.83 and 1.77 Ga. The similar ages and orientations of ~1.8 Ga dyke swarms in the NCC demonstrate that the amalgamated NCC experienced widespread extension at this time.

Based on the width statistics of dyke swarms on ten survey lines, an average crustal extension ratio of 0.35% was found for the NCC. The small magnitude of overall extension suggests that the mafic dyke swarms were emplaced into the elastic fractures, and indicates that the NCC had become a brittle plate prior to the emplacement of the mafic dyke swarms.

Precisely dated mafic dyke swarms, when used as paleostress indicators, can be employed in the paleostress field reconstruction of Precambrian cratons. Two dimensional finite element modeling (2-D FEM) of the NCC, in which the various blocks were assigned densities and elastic constants, shows that north–south compression favors dyke intrusion along generally N–NW lines, and that deviations in dyke trends can be explained by the effects of boundary constraints and the physical properties of the crust. The best fitting model can be considered a plausible representation of the tectonic force acting on the NCC that produces the intraplate stress field that is most consistent with the observed orientation of dyke swarms. The results of modeling of the Late Paleoproterozoic stress field suggest a common tectonic setting for the emplacement of mafic dyke swarms in the Central Orogenic Zone, Western and East Blocks of the NCC. The results also show that the north–south tectonic forces play an important role in determining the paleostress field in the NCC. The widespread extension of the NCC resulted from the north–south tectonic forces which may be related to the break-up of the Late Paleoproterozoic supercontinent. The paleostress field modeling provides a possible approach to consider the supercontinent paleostress reconstruction and to reveal the mechanisms of the supercontinent break-up.

Keywords: Crustal extension; Mafic dyke swarms; Aulacogens; Geochronology; Paleostress reconstruction; Finite element modeling

1. Introduction

The North China Craton was probably involved in the amalgamation and subsequent break-up of a Late Paleoproterozic supercontinent (Pre-Rodinia supercontinent) (Rogers and Santosh, 2002; Wilde et al., 2002; Zhao et al., 2002a,b, 2004). The Archaean North China

* Corresponding author. School of Earth and Space Sciences, Peking University, Beijing 100871, China.
E-mail address: gthou@pku.edu.cn (G. Hou).

0040-1951/$ - see front matter © 2006 Elsevier B.V. All rights reserved.
doi:10.1016/j.tecto.2006.05.008

Craton (NCC, Fig. 1) is separated into Eastern and Western Blocks by a tectonic feature known as the Central Orogenic Zone (COZ) (Zhao et al., 2000, 2001; Zhao, 2001; Kusky et al., 2001; Wilde et al., 2002; Kusky and Li, 2003). The precise origin of this feature is controversial; some workers believe it represents a collision between the two Archaean blocks at ~1.85 Ga (Zhao et al., 2000, 2001, Zhao, 2001; Zhao et al., 2002a, b; Wilde et al., 2002; Kröner et al., 2005), while others regard it as a zone of Paleoproterozoic reworking within a single craton subjected to an Andean-style collision along its northern margin (Zhai et al., 2000; Kusky et al., 2001; Li et al., 2001, 2002; Kusky and Li, 2003; Zhai et al., 2005). What is clear is the timing of the last phase of metamorphism prior to cratonization at about 1.90 to 1.85 Ga. Immediately following this metamorphism, and representing the first igneous activity on the craton, was the intrusion of mafic dykes and the eruption of associated volcanics. The volcanics accumulated in several fault-bounded troughs or aulacogens and are largely covered by younger Proterozoic sediments, deposited in these subsiding grabens while the dykes occur as generally N–NW trending swarms outside the grabens and within the crystalline shield (Fig. 1). The mafic dyke swarms are spread in the West Block, the Central Orogenic Zone and the East Block. The Late Paleoproterozoic marks a discrete change in the Precambrian evolution of the NCC as well as other cratons throughout the world.

Issues that require consideration in understanding the Proterozoic evolution of the NCC and the systematics of the initial break-up of the Pre-Rodinia supercontinent

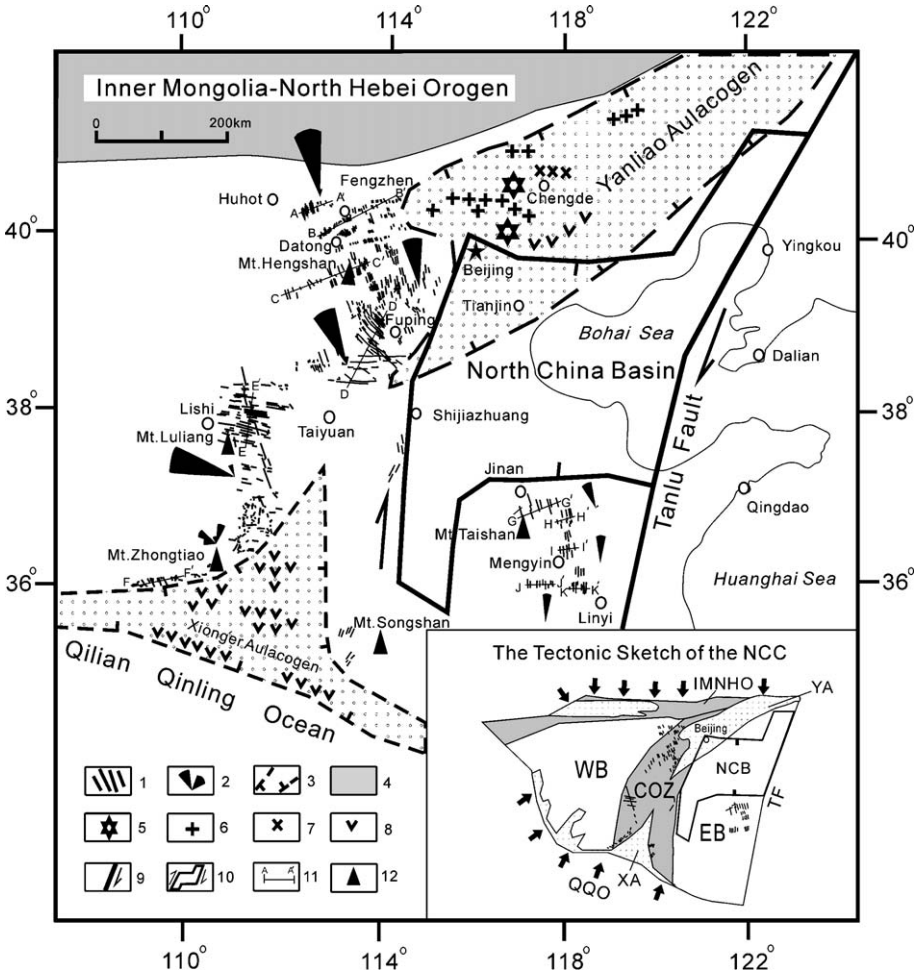

Fig. 1. Proterozoic aulacogens and mafic dyke swarms of the North China Craton. 1. Dyke swarms; 2. orientation roses; 3. aulacogen; 4. Late Paleoproterozoic Orogen; 5. rapakivi granite; 6. granite; 7. anorthosite; 8. volcanics; 9. Tanlu Fault; 10. Meso-Cenozoic pull-apart basin; 11. profile and name; 12. mount. WB — Western Block; COZ — Central Orogenic Zone; EB — Eastern Block; IMNHO — Inner Mongolia–North Hebei Orogen; QQO — Qilian–Qinling Orogen; NCB — North China Basin; TF — Tanlu Fault; XA — Xiongʼer Aulacogen; YA — Yanliao Aulacogen.

include: Whether the mafic dyke swarms in the West Block, Central Orogenic Zone and East Block were emplaced under the same crustal stress regime and what are the tectonic forces inducing the extension of the NCC? This paper provides a review of the current state of knowledge on the geochronology of the NCC and presents new data obtained from extension ratio calculations and a reconstruction of the paleostress field.

2. Geological background

The Paleoproterozoic NCC can be divided into three types of tectonic units, including the Archaean crystallization basements, the Paleoproterozoic orogens and the Late Paleoproterozoic–Mesoproterozoic aulacogens (Fig. 1). The Archaean crystallization basements include amphibolite facies gneiss in the West Block, TTG and adamellite in the East Block (Kusky and Li, 2003; Hou et al., 2004). The Paleoproterozoic orogens include the Inner Mongolia–North Hebei Orogen (IMNHO) in the northern margin of the NCC and the Central Orogenic Zone (COZ) in the central NCC (Fig. 1). The IMNHO includes the khondalites and high pressure granulite. The COZ includes the high pressure granulite and high amphibolite or amphibolite facies gneiss (Zhai et al., 2000; Zhao et al., 2000; Li et al., 2001, 2002; Wilde et al., 2002; Kusky and Li, 2003; Zhai et al., 2005). Yanliao and Xiong'er Aulacogens were filled by the Late Paleoproterozoic–Mesoproterozoic volcanic and sediments (Fig. 1) (Qian and Chen, 1987; Sun and Hu, 1993; Hou et al., 2000, 2001a,b; Zhao et al., 2002a,b).

In the Late Paleoproterozoic, the NCC was characterized by extensional structures such as aulacogens and mafic dyke swarms. Aulacogen systems and anorogenic magmatic belts occur mainly in the marginal areas of the NCC, whereas mafic dyke swarms were emplaced in the central portion of the craton. The extensional episode responsible for the formation of these extensional features also resulted in rapid cooling and final uplift and exposure of the NCC crystalline basement (Halls et al., 2000; Hou et al., 2000, 2001a,b, in press; Kusky and Li, 2003).

The volcanics from the Xiong'er Aulacogen give a U–Pb SHRIMP age of 1840±14 Ma, dating the opening of the southern arm of a three-pronged rift system (Sun and Hu, 1993; Zhao et al., 2002a,b). The Changcheng Series (including lava and sediments dated at 1.84 to 1.60 Ga) were filled in the Yanliao Aulacogen across the northern part of the NCC (Hu et al., 1997; Kusky and Li, 2003). Some Late Paleoproterozoic anorogenic intrusions (e.g. rapakivi granite and anorthosite) were also developed in the Yanliao Aulacogen (Xie and Wang, 1988; Yu, 1990; Li et al., 2001; Kusky and Li, 2003).

Dyke swarms developed in the NCC throughout the aulacogenic system in the Late Paleoproterozoic. The majority of dyke swarms in the NCC are distributed in the Shanxi Province of the Central Orogenic Zone and the West Block along the west of the Yanliao and Xiong'er Aulacogens, with a few also in the Shandong Province of the East Block (Chen and Shi, 1983; Qian and Chen, 1987; Halls et al., 2000; Hou et al., 2001a, 2004, 2005a). Unmetamorphosed mafic dyke swarms occur principally in four regions: The Datong–Hengshan–Fuping areas where they form the N–NW trending dyke swarms; the Luliang area where they form WNW and NNW trending dyke swarms; the Zhongtiao area where they form a radiating dyke swarm, and the Taishan area where they form N–NNW trending mafic dyke swarms (Fig. 1). Each of the dyke swarms is overlain by a generally flat-lying Neoproterozoic and/or Paleozoic sedimentary cover. Geological field relations thus constrain the age of the mafic dyke swarms to lie in Paleoproterozoic and Mesoproterozoic (Hou et al., 2005b).

Many precise ages of the Precambrian mafic dyke swarms in the NCC have been published in recent papers. Peng et al. (2005) gave a SHRIMP zircon U–Pb age of 1778±3 Ma for the mafic dyke swarms at Datong in the West Block of the NCC. A diabase dyke at Mt. Hengshan in the Central Orogenic Zone has yielded a single-grain zircon U–Pb age of 1769.1±2.5 Ga (Halls et al., 2000). Similarly, Liao et al. (2003) gave a ^{39}Ar–^{40}Ar age of 1780.7±0.5 Ma for a diabase dyke at Fuping in the Central Orogenic Zone. Shao et al. (2005) also gave a ^{39}Ar–^{40}Ar age of 1804±16 Ma for a mafic dyke at Mt. Hengshan and a ^{39}Ar–^{40}Ar age of 1725±16 Ma for a mafic dyke at Datong. Hou et al. (in press) gave a new SHRIMP zircon U–Pb age of 1830±17 Ma for a large mafic dyke at Mt. Taishan in the East Block. From the extensive previous geochronology it can be established that the ages of these mafic dyke swarms span between 1.83 Ga and 1.77 Ga.

These ages suggest that the widespread mafic dyke swarms of the NCC were emplaced at the same time as the cf. 1.8 Ga extensional event that followed cratonization of the NCC. Thus, the mafic dyke swarms and initial aulacogens in the NCC were developed in response to the same extensional event in the Late Paleoproterozoic.

These mafic dyke swarms maybe extend ~800 km in the West Block and Central Orogenic Zone, which are cut into several segments by narrow Cenozoic grabens. In the East Block, a 400 km-wide Meso-Cenozoic pull-apart basin, the North China Basin, developed between the Yanliao Aulacogen and the West Shandong (Mt. Taishan area), so the mafic dyke swarms in Mt. Taishan area were close to the Yanliao Aulacogen before Mesozoic (Hou et al., 2001b, 2005a).

3. A paleostress field reconstruction of the NCC

It is more difficult to reconstruct the paleostress field of Precambrian cratons than current stress field of plates due to few observed stress indicators in Precambrian cratons. The widespread Late Paleoproterozoic mafic dyke swarms in the NCC are regarded as excellent observed paleostress indicators. The Late Paleoproterozoic stress field of the NCC can be reconstructed based on the analysis of extensional structure and elastic finite element modeling.

3.1. Extension of the brittle NCC and emplacement of the mafic dyke swarms

About 640 mafic dykes of both N–NW and WNW trends are found in the NCC and are distributed within linear zones from 20 to 200 km in width. Individual dykes are vertical to sub-vertical, up to 10s of kilometers in length and from 5 to 100 m in width, with an average width of 10 m.

The mafic dykes are undeformed and unmetamorphosed with chilled margins that exhibit sharp contacts with the Archaean host rocks. The flow structures in the chilled margins and radial pattern show that the dyke swarms in the western NCC were emplaced northwestward from the Xiong'er and Yanliao Aulacogens (Hou et al., 2003). The mafic dyke swarms in the Zhongtiao area are also radially distributed and perpendicular to the western boundary of the Xiong'er Aulacogen. The mafic dyke swarms in the eastern NCC follow N–NNW trends, and flow structures suggest they were emplaced southward (Hou et al., 2005a).

Dyke swarms are regarded as valid markers for extension event. Crustal extension in the NCC was calculated based on the width statistics of dyke swarms on ten survey lines (Fig. 1). The formula $\lambda = \Sigma d_i/(L - \Sigma d_i)$ was employed in the calculation, where λ is the extension ratio; Σd_i is the total width of dykes on the survey line and L is the length of survey line cross the observed dyke swarms. Local extension ratios were calculated and are presented in Table 1. An average crustal extension ratio of 0.35% was found for the NCC, which was contributed by the mafic dyke swarms. The small magnitude of overall extension suggests that the mafic dyke swarms were emplaced as limited elastic fractures which formed an "upper crustal joint system" in the NCC, and indicates the NCC had become a brittle plate prior to the emplacement of the mafic dyke swarms.

The mafic dyke swarms of the NCC comprise quickly cooled intrusions of mafic magmas emplaced into a pre-existing fracture system. The pattern of dyke swarms and the shape of individual dykes are controlled by the mechanics of formation of the pre-existing fractures and thus the geometry of a dyke swarm can provide insight as to the original mechanics of formation of the dyke-hosting fractures (Pollard et al., 1987; Feraud et al., 1987; Ernst et al., 1995). Widespread parallel dyke swarms are generally considered to develop parallel to the contemporary maximum horizontal principal stress, a hypothesis that is strengthened by theoretical and experimental studies such as those of Pollard (1987). In general, dyke swarms with tensional form show their trends parallel to the regional compressive stress direction while their trends are perpendicular to the extension direction (Baer and Beyth, 1990; Hoek and Seitz, 1995; Gudmundsson, 1995; Heeremans et al., 1996).

Table 1
The calculation results of extension ratio on the Late Paleoproterozoic mafic dyke swarms of the NCC

Profile names	Length of profile (L) (m)	Total width of dykes (Σd_i) (m)	Extension ratio (λ) (%)	Region	Dominant orientation of dyke swarms
AA′	48,000	230	0.48	Datong	NNW
BB′	110,000	490	0.45	Datong	NNW
CC′	11,000	270	0.25	Hengshan	NNW
DD′	80,000	280	0.35	Fuping	NW
EE′	60,000	180	0.30	Luliang	WNW
FF′	60,000	190	0.32	Zhongtiao	NW
GG′	50,000	70	0.14	Taishan	NNW
HH′	20,000	80	0.40	Taishan	NNW
II′	20,000	60	0.30	Mengyin	NNW
JJ′	30,000	90	0.30	Linyi	SN
KK′	20,000	100	0.50	Linyi	SN
Average extension			0.35	NCC	

In the Mt. Hengshan area of the western NCC, most NNW trending mafic dyke swarms are vertical, with straight, well-defined margins and dextral offset segments, suggesting transtensional formation character of the pre-existing fractures. The mafic dyke swarms in other areas of the NCC are vertical and have irregular margins suggesting a tensional origin (Hou et al., 2003, 2005a).

Most mafic dyke swarms were emplaced in pre-existing tensional fractures with vertical and irregular boundaries, which display stable, parallel trends not controlled by the host rock lithology and occurrence. These characteristics suggest that the pre-existing fracture system into which the mafic dyke swarms intruded were formed in an extension regional stress field (Hou et al., 2001a, 2003). The orientations and density of dyke swarms can be used to determine the nature of the paleostress field, defining the horizontal principle stress directions and relative magnitudes (Price and Henry, 1984;

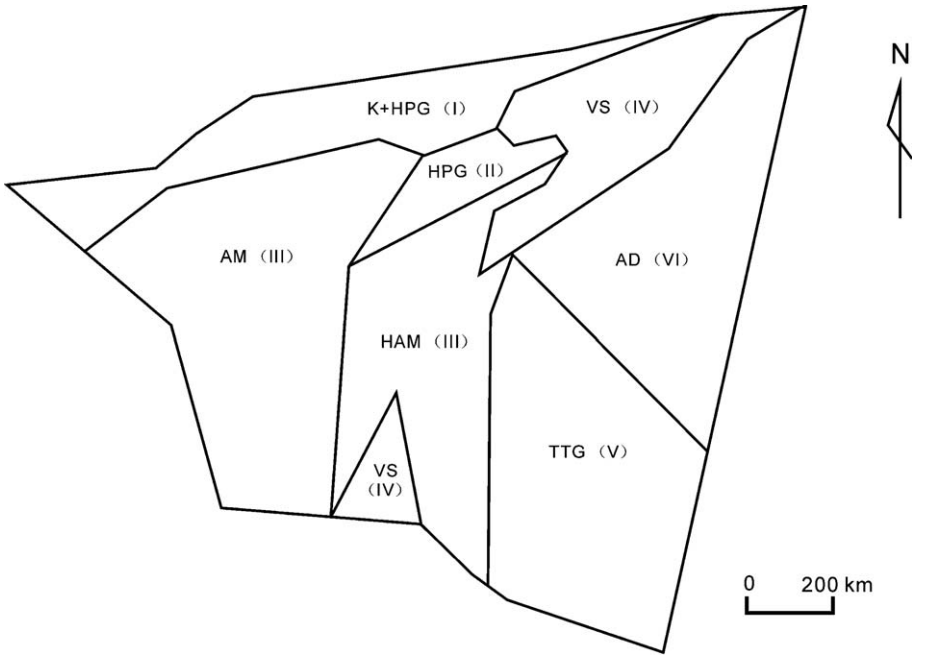

Fig. 2. The six different lithologic provinces of the linear elastic FEM of the NCC (after Kusky and Li, 2003; Hou et al., 2004, in press; Zhai et al., 2005).

Feraud et al., 1987; Hoek and Seitz, 1995). The Late Paleoproterozoic stress field can be reconstructed by elastic finite element models (FEM) based on the crustal characteristic of the NCC and the above-outlined hypothesis for dyke orientation as an indicator of the horizontal principle stress direction during formation. The quantitative modeling results rely on a qualitative assessment of the fit between predicted and observed stresses (e.g. the dyke swarms orientations).

3.2. Two dimensional finite element models (2-D FEM)

The Late Paleoproterozoic NCC was a rigid continental plate with extensive extension marked by mafic dyke swarms throughout the entire craton. The paleostress field can be reconstructed employing linear elastic theory. The FEM for the NCC was generated and stress trajectories were calculated using the ANSYS 8.0 (University Version) finite element software package. A more detailed description of the linear elastic finite element modeling technique can be found elsewhere (Richardson et al., 1979; Coblentz and Richardson, 1995).

The results of previous studies were used to constrain the FEM of the Late Paleoproterozoic NCC (Zhao et al., 2000; Wilde et al., 2002; Kusky and Li, 2003; Zhai and Liu, 2003; Hou et al., 2004, in press; Zhai et al., 2005). The NCC crust was modeled by its subdivision into six lithologically unique provinces (Figs. 1 and 2), to which appropriate densities and elastic constants were assigned (Lama and Vutukuri, 1978; Wang et al., 1983) (Table 2). The six lithological provinces, each representing a separate tectonic unit, include: A khondalite province (I); a high pressure granulite province (II); a high amphibolite-amphibolite facies gneiss province (III); an aulacogenic volcanics and sediments province (IV); a TTG province (V), and an adamellite province (VI) (Fig. 2). The five Archaean metamorphosed rock provinces (I–III and V–VI) are of similar elastic properties and competent in

Table 2
Elastic rock properties employed in the 2-D FEM for the North China Craton (Sources: Lama and Vutukuri, 1978; Wang et al., 1983)

Rock provinces (lithology)	Average density (kg/m^3)	Young's modulus (GPa)	Poisson's ratio
Khondalites+high pressure granulite (I)	2650	70	0.25
High pressure granulite (II)	2850	80	0.25
High amphibolite or amphibolite facies gneiss (III)	2550	70	0.25
Aulacogenic volcanics and sediments (IV)	2400	30	0.20
TTG (V)	2750	80	0.25
Adamellite (VI)	2800	80	0.25

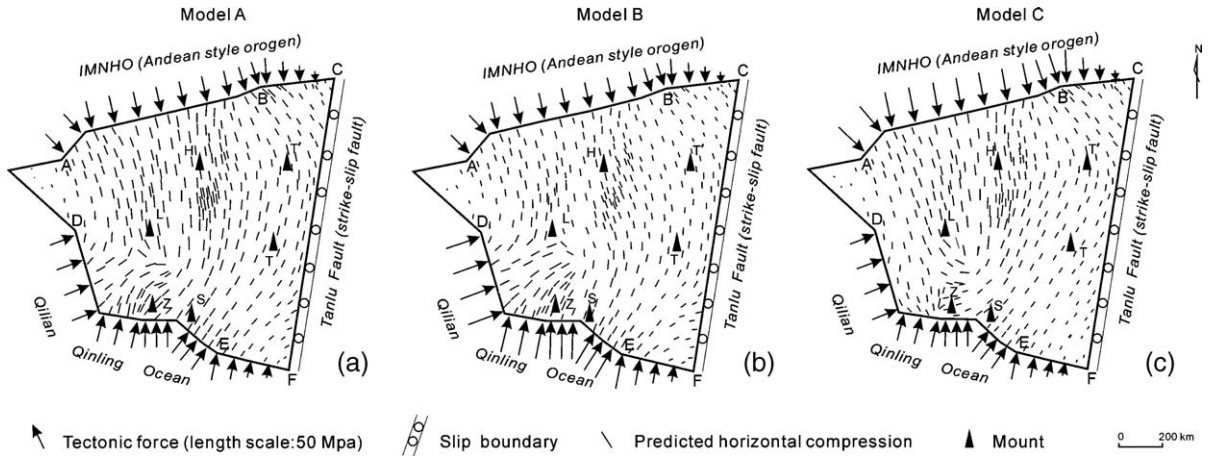

Fig. 3. The maximum principal stress (σ_{Hmax}) trajectory maps of top three models for the Late Paleoproterozoic North China Craton Arrow indicates the tectonic force and their length represents the data quality; fine bars in the NCC indicate the maximum principle stress vectors (σ_{Hmax}); (a) equal tectonic forces to the north and south boundaries; (b) bigger tectonic forces to the south than the north boundaries; (c) bigger tectonic forces to the north than the south boundaries H: location of Mt. Hengshan; L: location of Mt. Luliang; Z: location of Mt. Zhongtiaoshan; S: location of Mt. Songshan; T: location of Mt. Taishan; T′: location of Mt. Taishan before Mesozoic.

comparison to the aulacogenic volcanics and sediments province (IV). The average density of volcanic and sedimentary fill was taken as 2400 kg/m^3, and a Young's modulus of 30 GPa was assumed, values much different from those of the other rocks.

3.3. Constraints on the NCC

In the Late Paleoproterozoic, following cratonization, the NCC was a stable continent with triangular form bounded by the Qilian–Qinling Ocean (QQO) along its southern boundary, which is a passive continental margin, an Andean-style orogen (IMNHO) along its northern boundary and the Tanlu Fault (TLF) in its eastern boundary, which is a NNE-trending strike-slip fault (Fig. 1) (Kusky and Li, 2003; Hou et al., in press). The NE trending Yanliao Aulacogen and NNE trending Xiong'er Aulacogen stretched into the interior of the NCC (Fig. 1). Constraints placed on each boundary for the 2-D Finite Element Modeling of the NCC were based on the tectonic context of the NCC, described above.

In most continental areas such as stable North America and Australia, the maximum horizontal compressive stress (σ_{Hmax}) orientation occurs broadly parallel to the direction of plate motion and plate boundary forces exert the principal control on the character of the first-order intraplate stress field. This is confirmed by present-day regional stress field modeling (Richardson et al., 1979; Richardson and Reding, 1991; Richardson, 1992; Coblentz and Richardson, 1995, 1996; Reynolds et al., 2002). For the purpose of the FEM experiments, appropriate compressive forces were applied normal to the northern, southern and southwestern boundaries of the craton with a transform style eastern boundary, as shown in Fig. 3 (the transform style boundary can be constrained by roller displacement). The tectonic forces applied to the different boundaries are represented in Table 3. Stress magnitudes of ~50 MPa were found in continents from fieldwork for considering boundary constraint (Reynolds et al., 2002; Chatterjee and Mukhopadhyay, 2002).

3.4. Modeling results and discussion

Orientations of the tectonic paleostress in the NCC were predicted using a two-dimensional elastic finite element analysis. The NCC crust was regarded as an elastic flat plate whose thickness is 1. The finite element grid consisted of 392 triangular elements, each defined by 6 nodes for a total of 444 nodes. It should be noted that the sensitivity of the modeled stresses was therefore limited to large-scale tectonic features with wavelengths of a few ten kilometers. The stress trajectories of the top

Table 3
Tectonic force magnitudes applied to the different boundaries for top three models

Model	Tectonic force magnitudes applied to the different boundaries (MPa)				Results
	AB	BC	DE	EF	
Model A	50	50→0	50	50→0	Fig. 3a
Model B	50	50→0	70	70→0	Fig. 3b
Model C	70	70→0	50	50→0	Fig. 3c

50→0 represents that tectonic forces decompress gradually from 50 to 0 MPa.

three models are given in Fig. 3, which are three much better fitting models in the hundreds of experiments. Information on the stress magnitude was not included in the calculation due to the lack of stress regime data in the observed stress indicators.

Reasonable modeling results of paleostress fields rely on the qualitative fit between calculated and observed stresses (Reynolds et al., 2002; Chatterjee and Mukhopadhyay, 2002). A method of measurement of the success of a FEM is to match the maximum stress trajectories with the mafic dyke swarms orientations. Eight rose diagrams of the mafic dyke swarms were used as observed stress indicators to constrain the calculated stress field (Fig. 1).

The stress patterns in the NCC are divided into five stress provinces with different patterns: The Mt. Hengshan area (H), the Mt. Luliang area (L), the Mt. Zhongtiao area (Z), the Mt. Songshan area (S) and the Mt. Taishan area (T) (Fig. 3). T′ represents the location of Taishan area before Mesozoic.

Firstly, we see Model A (Table 3 and Fig. 3a), in which the tectonic forces are equally applied along the north and south boundaries of NCC. In the Mt. Hengshan area (H), west of the aulacogens, the maximum horizontal compressive stresses (σ_{Hmax}) are N–S trending, about 20°–30° (angles between dyke orientations and σ_{Hmax} vectors) off the trend of the NNW trending dyke swarms of the region, possibly due to the transtensional character of the pre-existing fractures intruded by the mafic dyke swarms (Figs. 1 and 3a). In the Mt. Luliang area (L), σ_{Hmax} orientations are NW and trends parallel to the principle compression which produces the joint dyke swarms (WNW trending and NNW trending dykes) in the western Taiyuan, due to closing the terminals of two aulacogens (Figs. 1 and 3a). In the southern Shijiazhuang, σ_{Hmax} orientations fit well to the orientation of the dyke swarms (Figs. 1 and 3a). In the Mt. Songshan area (S), σ_{Hmax} orientations trend NE and fit well to the trend of the dyke swarms (Figs. 1 and 3a). In the Mt. Taishan area (T), σ_{Hmax} orientations are N–NNW, but do not fit well with the orientation of the mafic dyke swarms. The σ_{Hmax} orientations fit well with the orientations of the dyke swarms in the area T′ before the Mesozoic after reconstruction (Figs. 1 and 3a). The rotation of σ_{Hmax} orientations from NNW trend in the northern Taishan to N trend in the southern Taishan may be controlled by the strike-slip Tanlu Fault that forms the eastern boundary of the NCC.

Except the Mt. Zhongtiao area (Z), the stress trajectory map fit well with the orientations of mafic dyke swarms in different provinces (Fig. 3a). σ_{Hmax} orientations trend NE in the Zhongtiao area (Z) in the Model A, but the mafic dyke swarms trend N–NW, NE and E–W in the area Z (Figs. 1 and 3a).

Secondly, we see Model B (Fig. 3b), in which the tectonic forces on the south boundary are stronger than the forces applied on the north boundary of NCC (Table 3). The misfit between the modeled σ_{Hmax} and dyke orientations in area Z is still not resolved in Model B though the results fit well in the other areas (Fig. 3b).

Finally, we see Model C (Fig. 3c), in which the tectonic forces on the north boundary are stronger than the forces applied on the south boundary of NCC (Table 3). In this model, the best fitting results are achieved (Fig. 3c). The results in Fig. 3c are broadly similar to the results in Fig. 3a and b in the most of NCC except the Mt. Zhongtiao area (Z). In Model C, σ_{Hmax} trend N–NW, NE and E–W in a radiating pattern (Fig. 3c). The σ_{Hmax} vectors fit very well to the radiating dyke swarm orientations in the area Z (Fig. 1).

The stress trajectories are more densely concentrated near the west of the two aulacogens due to the intersection at that point of the different tectonic units and triangle boundaries in the West Block and Central Orogenic Zone (e.g. Mt. Hengshan area and Mt. Zhongtiao area) (Fig. 3). Most σ_{Hmax} orientations in the stress vector plot are well fitted to the mafic dyke swarms trends throughout the NCC. The stress trajectories are continuous in the Archaean crystalline basement due to the similar elastic properties in the different lithological provinces, except for the sizable contrast between the elastic properties in the basement and in the aulacogens.

Model C is the best fitting model among the top three models. The results presented in Model C provide a good fit to the observed paleostress indicators (e.g. dyke swarms) throughout the entire NCC. Our modeling results indicate that a good fit to the orientations of dyke swarms in area Z requires stronger compression along the north boundary than the south boundary of NCC. About 40% difference between the forces along the north and south boundaries can result in a significant change in the predicted σ_{Hmax} orientations for area Z. The comparisons between the top three models suggest that the observed paleostress field in area Z plays a critical role in determining the relative force magnitude along the north and south boundaries (Fig. 3 and Table 3).

Model C is more tectonically plausible than the other models. The tectonic forces are stronger on the north boundary than the south boundary (Table 3 and Fig. 3c). The tectonic forces along the north boundary are dominant in the boundary constraints. This assumption is supported by previous tectonic studies. The north boundary is a Late Paleoproterozoic Andean-style Orogen whose collision resulted in the exhumation of a 700-km long high pressure granulite belt in the northern NCC, while the south boundary is a passive continental

boundary (Zhai et al., 2000; Kusky et al., 2001; Li et al., 2001, 2002; Kusky and Li, 2003; Zhai et al., 2005).

The top three fitting models (Fig. 3), show maximum stress trajectories that swing from N–NW in the northwest toward more southerly trends to the N–NE, possibly due to the coupling between the north–south forces and the eastern strike-slip boundary (Figs. 1 and 3). The modeled stress field in the NCC is highly sensitive to changes in the forces applied to the craton boundaries. The results suggest that the dyke swarms in the West Block, Central Orogenic Zone and the East Block represent coeval extensional structures in the NCC, controlled by the same stress field in the Late Paleoproterozoic.

Factors affecting the modeling results of modeling of the paleostress field include the nature of the applied tectonic forces, the shape of the NCC, the geometrical configuration outlining of the aulacogens, the behaviour of the eastern boundary (strike-slip or not strike-slip) and the value of the different elastic properties assigned to the NCC. The results of finite element modeling of the NCC indicate that the north–south tectonic forces play a major role in determining the paleostress field in the NCC. The comparisons between three models suggest that tectonic forces control the regional intraplate stress field of the NCC. Furthermore, boundary shape and lithological properties also affect the stress pattern. The elastic properties of different rock units less influence the modeling results due to the similarity of the different Archaean crystallization basements in Young's modulus and Poisson's ratio.

4. Conclusions

The North China Craton became a rigid craton after the cratonization at ~1.85 Ga. The Xiong'er Aulacogen developed Xiong'er Group volcanic rocks stretching to interior from the southern NCC as a triple junction (1.84 Ga), while the Yanliao aulacogen was filled with aulacogenic volcanics and sedimentary rocks (1.84–1.60 Ga). The mafic dyke swarms cutting all of the Neoarchean and Early Paleoproterozoic terrains mainly span from 1.83 to 1.77 Ga. An average extension ratio of 0.35% was calculated for the extension related to the mafic dyke swarms. This suggests that the mafic dyke swarms are just a very limited crustal fissure system and the mafic dyke swarms possibly mark the start of a Late Paleoproterozoic supercontinent break-up.

The modeling results of Late Paleoproterozoic stress field of the NCC suggest the mafic dyke swarms in the Central Orogenic Zone, the Western and Eastern Blocks were formed in the same tectonic setting. These dyke swarms throughout the NCC are related to the same extensional episode in the Late Paleoproterozoic. Tectonic forces and the boundary shape play important roles in determining paleostress trajectories. The comparisons between the top three fitting models suggest that north–south tectonic forces control the regional intraplate stress field in the NCC. The best fitting model indicates that the tectonic forces are stronger along the north boundary than the south boundary of the NCC. The best model, while nonunique, can be considered to be a plausible representation of the tectonic constraint on the boundaries of the NCC. Compressional forces act along the north and south boundaries to produce stress focusing normal to these boundaries and stress rotation in a triangle area.

Similar Late Paleoproterozoic dyke swarms to that discussed in this paper are also found in the South India Craton and the western Canadian Shield (Giddings, 1976; Buchan and Halls, 1990; Okrugin et al., 1990; Boyd and Tucker, 1990; Rao et al., 1990; Radhakrishna et al., 1999; Griffin et al., 1999). It may be useful to reconstruct a mantle superplume position of supercontinental break-up by comparing the mafic dyke swarms of different cratons throughout the world. The coeval dyke swarms in the NCC and other cratons mentioned above suggest that the North China Craton may represent a part of a Pre-Rodinia supercontinent. The tectonic forces on the Late Paleoproterozoic NCC perhaps came from the break-up of the Pre-Rodinia supercontinent, and induced the intraplate extension of the NCC (e.g. N–NNW trending mafic dyke swarms). The modeling results tell us that the mafic dyke swarms did not directly result from the break-up of a supercontinent, but were induced from the north–south tectonic forces given by oceanic spreading during the break-up episode of the supercontinent.

Precisely dated mafic dyke swarms, when used as paleostress indicators, can become conspicuous tectonic markers for the reconstruction of supercontinents. Paleostress field modeling provides a possible approach to consider the supercontinent paleostress reconstruction and to reveal mechanisms of supercontinent break-up.

Acknowledgement

Thanks for Prof. Henry C Halls' review that improved the paper and Prof. Gordon S. Lister's fruitful discussion, thanks to Daniel R. Viete for going through the paper word by word. Thanks to Prof. H. Liang for giving useful suggestion for the digital experiment. Thanks to two anonymous reviewers who gave constructive reviews of the manuscript. This work was supported by funds from the National Natural Science Foundation of China (Grant No. 40172066 and 40314141) and the Peking University–ANU Exchange Project.

References

Baer, G., Beyth, M., 1990. A mechanism of dyke segmentation in fractured host rock. In: Parker, A.J., Rickwood, R.C., Tucker, D.H. (Eds.), Mafic Dykes and Emplacement Mechanisms. Balkema, Rotterdam, pp. 3–11.

Boyd, D.M., Tucker, D.H., 1990. Australian magnetic dykes. In: Parker, A.J., Rickwood, P.C., Tucker, D.H. (Eds.), Mafic Dykes and Emplacement Mechanisms. Balkema, Rotterdam, pp. 391–400.

Buchan, K.L., Halls, H.C., 1990. Paleomagnetism of Proterozoic mafic dyke swarms of the Canadian Shield. In: Parker, A.J., Rickwood, P.C., Tucker, D.H. (Eds.), Mafic Dykes and Emplacement Mechanisms. Balkema, Rotterdam, pp. 209–230.

Chatterjee, R., Mukhopadhyay, M., 2002. Effects of rock mechanical properties on local stress field of the Mahanadi basin, India-results from finite element modeling. Geophys. Res. Lett. 29 (11), 28-1–28-4.

Chen, X.D., Shi, L.B., 1983. Primary research on the diabase dyke swarms in Wutai–Fuping area. Chin. Sci. Bull. 16, 1002–1005.

Coblentz, D.D., Richardson, R.M., 1995. Statistical trends in the intraplate stress field. J. Geophys. Res. 100 (B10), 20, 245–20, 255.

Coblentz, D.D., Richardson, R.M., 1996. Analysis of the South American intraplate stress field. J. Geophys. Res. 101 (B4), 8643–8657.

Ernst, R.E., Buchan, K.L., Palmer, H.C., 1995. Giant dyke swarms: characteristics, distribution and geotectonic applications. In: Baer, G., Heimann, A. (Eds.), Physics and Chemistry of Dykes. Balkema, Netherlands, pp. 1–21.

Feraud, G., Giannerini, G., Campredon, R., 1987. Dyke swarms as paleostress indicators in areas adjacent to continental collision zones: examples from the European and Northwest Arabian plates. In: Halls, H.C., Fahrig, W.F. (Eds.), Mafic Dyke Swarms. Geological Association of Canada Special Paper, vol. 34, pp. 273–278.

Giddings, J.W., 1976. Precambrian palaeomagnetism in Australia. I. Basic dykes and volcanics from the Yilgarn Block. Tectonophysics 30, 91–108.

Griffin, W.L., Ryan, C.G., Kaminsky, F.V., Suzanne, Y.O., Natapov, L.M., Win, T.T., Kinny, P.D., Ilupin, I.P., 1999. The Siberian lithosphere traverse: mantle terranes and the assembly of the Siberian Craton. Tectonophysics 310, 1–35.

Gudmundsson, A., 1995. The geometry and growth of dykes. In: Baer, G., Heimann, A. (Eds.), Physics and Chemistry of Dykes. Balkema, Rotterdam, pp. 23–34.

Halls, H.C., Li, J.H., Davis, D., Hou, G.T., Qian, X.L., 2000. A precisely dated Proterozoic palaeomagnetic pole from the North China Craton, and its relevance to palaeocontinental reconstruction. Geophys. J. Int. 143, 185–203.

Heeremans, M., Larsen, B., Stel, H., 1996. Paleostress reconstruction from kinematic indicators in the Oslo Graben, southern Norway: new constraints on the mode of rifting. Tectonophysics 266, 55–79.

Hoek, J.D., Seitz, H.M., 1995. Continental mafic dyke swarms as tectonic indicators: an example from the Vestfold Hills, East Antarctia. Precambrian Res. 75, 121–139.

Hou, G.T., Li, J.H., Qian, X.L., 2000. The paleomagnetism of dyke swarms in the central North China Craton and their tectonic significance. Sci. China, Ser. D: Earth Sci. 30 (6), 602–608.

Hou, G.T., Li, J.H., Qian, X.L., 2001a. Geochemical characteristics and tectonic setting of Mesoproterozoic dyke swarms in northern Shanxi. Acta Petrol. Sin. 17 (3), 352–357.

Hou, G.T., Qian, X.L., Cai, D.S., 2001b. The tectonic evolution of Bohai Basin in Mesozoic and Cenozoic time. Acta Scientiarum Naturalium Universitatis Pekinensis, vol. 37 (6), pp. 845–851.

Hou, G.T., Li, J.H., Qian, X.L., 2003. The flow structures and mechanics of Late Precambrian mafic dyke swarms in North China Craton. Acta Geol. Sin. 77 (2), 210–216.

Hou, G.T., Li, J.H., Jin, A.W., Qian, X.L., 2004. The new comment on the division and evolution of Early Precambrian tectonic magmatism in the western Shandong. Geol. J. Chin. Univ. 10 (2), 239–249.

Hou, G.T., Liu, Y.L., Li, J.H., Qian, X.L., 2005a. The mafic dyke swarms in the western Shandong. Acta Geol. Sin. 79 (2), 190–199.

Hou, G.T., Liu, Y.L., Li, J.H., Jin, A.W., 2005b. The discussion on the U–Pb SHRIMP dating of mafic dyke swarms. Acta Petrol. Mineral. Sin. 24 (3), 179–185.

Hou, G.T. Liu, Y.L., Li, J.H., Qian, X.L., in press. Evidence for ~1.8 Ga extension of the East Block of the North China Craton from SHRIMP U–Pb dating of mafic dyke swarms in Shandong Province. J. Asian Earth Sci.

Hu, X.D., Chen, Z.H., Zhao, Y.M., 1997. Age of Xiaoyingpan gold ore: new evidence from the single zircon U–Pb isotopic dating. Prog. Precambrian Res. 20 (2), 22–28.

Kröner, A., Wilde, S.A., Li, J.H., Wang, K.Y., 2005. Age and evolution of a Late Archean to Early Paleoproterozoic upper to lower crustal section in the Wutaishan/Hengshan/Fuping terrain of northern China. J. Asian Earth Sci. 24 (5), 577–595.

Kusky, T.M., Li, J.H., 2003. Paleoproterozoic tectonic evolution of the North China Craton. J. Asian Earth Sci. 22, 383–397.

Kusky, T.M., Li, J.H., Tucker, R.T., 2001. The Archaean Dongwazi ophiolite complex, North China Craton: 2.505 billion year old oceanic crust and mantle. Science 292, 1142–1145.

Lama, R.D., Vutukuri, V.S., 1978. Handbook on Mechanical Properties of Rocks — Testing Techniques and Result — Vol. II. Tarns Tech Publication, Switzerland, pp. 315–453.

Li, J.H., Hou, G.T., Huang, X.N., Zhang, Z.Q., Qian, X.L., 2001. Precambrian geology of North China Block. Acta Petrol. Sin. 17 (2), 177–186.

Li, J.H., Kusky, T.M., Huang, X.N., 2002. Neoarchaean podiform chromitites and mantle tectonites in ophiolitic melange, North China Craton: a record of early oceanic mantle processes. GSA Today 12, 4–11.

Liao, C.L., Wang, Y.J., Peng, T.P., 2003. $^{40}Ar/^{39}Ar$ geochronology and their tectonic significance of Early Proterozoic mafic dykes in the southern Fupingshan. Tecton. Mineral. 27, 354–360.

Okrugin, A.V., Oleinikov, B.V., Savvinov, V.T., Tomshin, M.D., 1990. Late Precambrian dyke swarms of the Anabar Massif, Siberian Platform. In: Parker, A.J., Rickwood, P.C., Tucker, D.H. (Eds.), Mafic Dykes and Emplacement Mechanisms. Balkema, Rotterdam, pp. 529–533.

Peng, P., Zhai, M.G., Zhang, H.F., Guo, J.H., 2005. Geochronological constraints on the Paleoproterozoic evolution of the North China Craton: SHRIMP zircon ages of different types of mafic dykes. Int. Geol. Rev. 47, 492–508.

Pollard, D.D., 1987. Elementary fracture mechanics applied to the structural interpretation of dykes. In: Halls, H.C., Fahrig, W.H. (Eds.), Mafic Dyke Swarms. Geological Association of Canada Special Paper, vol. 34, pp. 5–24.

Price, J.G., Henry, C.D., 1984. Stress orientations during Oligocene volcanism in Trans-Pecos Texas: timing the transition from Laramide compression to basin and range tension. Geology 12, 238–241.

Qian, X.L., Chen, Y.P., 1987. Late Precambrian mafic dyke swarms of the North China Craton. In: Halls, H.C., Fahrig, W.F. (Eds.), Mafic Dyke Swarms. Geological Association of Canada Special Paper, vol. 34, pp. 385–392.

Radhakrishna, T., Maluski, H., Mitchell, J.G., Joseph, M., 1999. $^{40}Ar/^{39}Ar$ and K/Ar geochronology of the dykes from the south Indian granulite terrain. Tectonophysics 304, 109–129.

Rao, J.M., Rao, G.S., Patil, S.K., 1990. Geochemical and paleomagnetic studies on the Middle Proterozoic Karimnagar mafic dyke swarms, India. In: Parker, A.J., Rickwood, P.C., Tucker, D.H. (Eds.), Mafic Dykes and Emplacement Mechanisms. Balkema, Rotterdam, pp. 373–382.

Reynolds, S.D., Coblentz, D.D., Hillis, R.R., 2002. Tectonic forces controlling the regional intraplate stress field in continental Australia: Results from new finite element modeling. J. Geophys. Res. 107 (B7) (1,1-15).

Richardson, R.M., 1992. Ridge forces, absolute plate motions, and the intraplate stress field. J. Geophys. Res. 97 (B8), 11, 739–11, 748.

Richardson, R.M., Reding, L.M., 1991. North American plate dynamics. J. Geophys. Res. 96 (B7), 12, 201–12, 223.

Richardson, R.M., Solomon, S.C., Sleep, N.H., 1979. Tectonic stress in the plates. Rev. Geophys. 17 (5), 981–1019.

Rogers, J.J.W., Santosh, M., 2002. Configuration of Columbia, a Mesoproterozoic supercontinent. Gondwana Res. 5, 123–132.

Shao, J.A., Zhai, M.G., Zhang, D.M., et al., 2005. Identification of 5 time-groups of dike swarms in Shanxi–Hebei–Inner Mongolia border area and its tectonic implications. Acta Geol. Sin. 79 (1), 56–67.

Sun, D.Z., Hu, W.X., 1993. The Age Framework and Crust Texture of Precambrian Mountain Zhongtiao Area. Geological Publishing House, Beijing, pp. 79–117.

Wang, R., Ding, Z.Y., Yin, Y.Q., 1983. Physical Solid Mechanics. Geological Press House, Beijing, pp. 201–208.

Wilde, S.A., Zhao, G.C., Sun, M., 2002. Development of the North China Craton during the Late Archean and its amalgamation along a major 1.8 Ga collision zone: including speculations on its position within a global paleoproterozoic supercontinent. Gondwana Res. 5, 85–94.

Xie, G.H., Wang, J.W., 1988. Primary research on the age of Damiao anorthosite complex. Geochim. Sin. 1, 13–16.

Yu, J.H., 1990. The geochemistry of the anorogenic rapakivi granite in the Proterozoic aulacogenin Beijing area. Acta Geol. Sin. 4, 322–335.

Zhai, M.G., Liu, W.J., 2003. Paleoproterozoic tectonic history of the North China Craton: a review. Precambrian Res. 122, 183–199.

Zhai, M.G., Bian, A.G., Zhao, T.P., 2000. The amalgamation of the supercontinent of North China Craton at the end of the Neoarchean, and its break-up during the Late Paleoproterozoic and Mesoproterozoic. Sci. China, Ser. D: Earth Sci. 43, 219–232 (Supp.).

Zhai, M.G., Guo, J.H., Liu, W.J., 2005. Neoarchean to Paleoproterozoic continental evolution and tectonic history of the North China Craton: a review. J. Asian Earth Sci. 24, 547–561.

Zhao, G.C., 2001. Paleoproterozoic assembly of the North China Craton. Geol. Mag. 138 (1), 89–91.

Zhao, G.C., Cawood, P.A., Wilde, S.A., Sun, M., Lu, L., 2000. Metamorphism of basement rocks in the central zone of the North China Craton: implications for Paleoproterozoic tectonic evolution. Precambrian Res. 103, 55–88.

Zhao, G.C., Wilde, S.A., Cawood, P.A., Sun, M., 2001. Archean blocks and their boundaries in the North China Craton: lithological, geochemical, structural and *P–T* path constraints and tectonic evolution. Precambrian Res. 107, 45–73.

Zhao, G.C., Cawood, P.A., Wilde, S.A., Sun, M., 2002a. Review of global 2.1–1.8 Ga orogens: implications for a pre-Rodinia supercontinent. Earth-Sci. Rev. 59, 125–162.

Zhao, T.P., Zhou, M.F., Zhai, M.G., 2002b. Paleoproterozoic rift-related volcanism of the Xiong'er group, North China Craton: implications for the breakup of Columbia. Int. Geol. Rev. 44, 336–351.

Zhao, G.C., Sun, M., Wilde, S.A., Li, S.Z., 2004. A Paleo-Mesoproterozoic supercontinent: assembly, growth and breakup. Earth-Sci. Rev. 67, 91–123.